Supplementary Information for: *Underestimated risks of future storm surge extremes: A global study*

Peter Thejll et al.

November 18, 2025

Contents

1. Results for non-stationary locations

Table 1: Tide-gauge stations that show statistically significant non-stationarity in the location parameter of the extreme-value distribution. Columns (1)-(4) identify the station, (5) is the length of the data series in years, (6) is the likelihood ratio test p value. Column (7) gives the coefficient of the covariate in the non-stationary GEV model, and (8) is the difference in AIC between stationary and non-stationary GEV model.

Station (1)	Country (2)	lon (3)	lat (4)	N (5)	p (6)	β (7)	ΔAIC (8)
Buenos Aires	ARG	-58.50	-34.67	57	0.00009	2.3	13.3
Albany	AUS	117.89	-35.03	55	0.02575	0.3	3.0
Newcastle	AUS	151.79	-32.92	56	0.00243	-0.6	7.2
Buenaventura	COL	-77.06	3.89	62	0.04681	-0.7	1.9
Tumaco	COL	-78.73	1.82	68	0.04455	-1.1	2.0
Cuxhaven	DEU	8.72	53.87	102	0.00086	2.4	9.1
Esbjerg	DNK	8.43	55.47	71	0.00218	1.6	7.4
La Libertad	ECU	-80.92	-2.20	70	0.00620	-0.1	5.5
Newlyn Cornwall	GBR	-5.54	50.10	102	0.00170	-0.5	7.9
Fukue	JPN	128.85	32.70	56	0.00339	-0.6	6.6
Mera	JPN	139.82	34.92	55	0.02967	0.4	2.7
Okada	JPN	139.39	34.79	60	0.01998	-0.5	3.4
Tokuyama	JPN	131.80	34.04	70	0.02520	-0.4	3.0
Kwajalein	MHL	167.73	8.73	73	0.00131	-0.2	8.3
Bergen	NOR	5.32	60.40	103	0.00042	0.7	10.4
Bodo	NOR	14.40	67.29	71	0.01421	1.1	4.0
Harstad	NOR	16.55	68.80	69	0.00113	0.8	8.6
Narvik	NOR	17.43	68.43	81	0.00247	0.7	7.2
Oscarsborg	NOR	10.60	59.68	68	0.02160	0.7	3.3
Tromso	NOR	18.95	69.65	69	0.01959	0.5	3.4
Furuogrund	SWE	21.23	64.92	105	0.00000	-0.3	18.9
Goteborg Torshamnen	SWE	11.79	57.68	55	0.00115	1.6	8.6
Kungsholmsfort	SWE	15.59	56.11	136	0.00268	0.8	7.0
Stenungsund	SWE	11.83	58.09	58	0.00197	1.4	7.6
Apra Harbor Guam	USA	144.65	13.43	70	0.00370	-0.1	6.4
Eastport	USA	-66.98	44.90	93	0.02980	-0.3	2.7
La Jolla	USA	-117.26	32.87	98	0.00116	-0.3	8.6
Mayport Ferry Depot	USA	-81.43	30.39	73	0.03700	0.4	2.4
Providence	USA	-71.40	41.81	76	0.00898	-0.9	4.8
San Diego	USA	-117.17	32.71	116	0.00057	-0.3	9.9
San Francisco Ca	USA	-122.47	37.81	122	0.00300	0.3	6.8
Sitka	USA	-135.34	57.05	84	0.00505	0.3	5.9
Wake Island	USA	166.62	19.29	71	0.01736	-0.2	3.7
Yakutat Ak	USA	-139.74	59.55	58	0.00051	0.2	10.1

2. Supplementary Figures

SI Figures 1–11. Statistically significant non-stationary stations. Each figure shows three panels: (left) annual mean sea level trends; (middle) scatterplots of residual extremes vs MSL with a fitted slope (β); (right) the bootstrapped distribution of β for each station. Figures are grouped by geographic region and shown only for stations where the β parameter is statistically significant at the 5% level.

SI Figure 12. Illustrating that stations can have positive or negative MSL trends and residuals with either slope vs MSL.

SI Figures 13–16. Showing bathymetric details around each station. Rings are at 1, 5 and 15 km radius.

SI Figures 17. Median depths and slopes near non-stationary stations.

3. Omitted GESLA series

Among the ocean-coast GESLA data are several that reveal quality issues when inspected. Instead of guessing how to fix some of them (e.g. those with a sharp clear offset in a year) we decided to eliminate such series from analysis. These include Izuhara, Naze, Maisaka, Ominato, Aomorika, Hanasaki, Kamaishi, Kobe, Kozushima, Onahama, Tokyo. Landsort in Sweden has two long series with quite different slope against time, but is otherwise good. Churchill, Canada is eliminated due to concerns over a climate signal entering through retreat of winter ice.

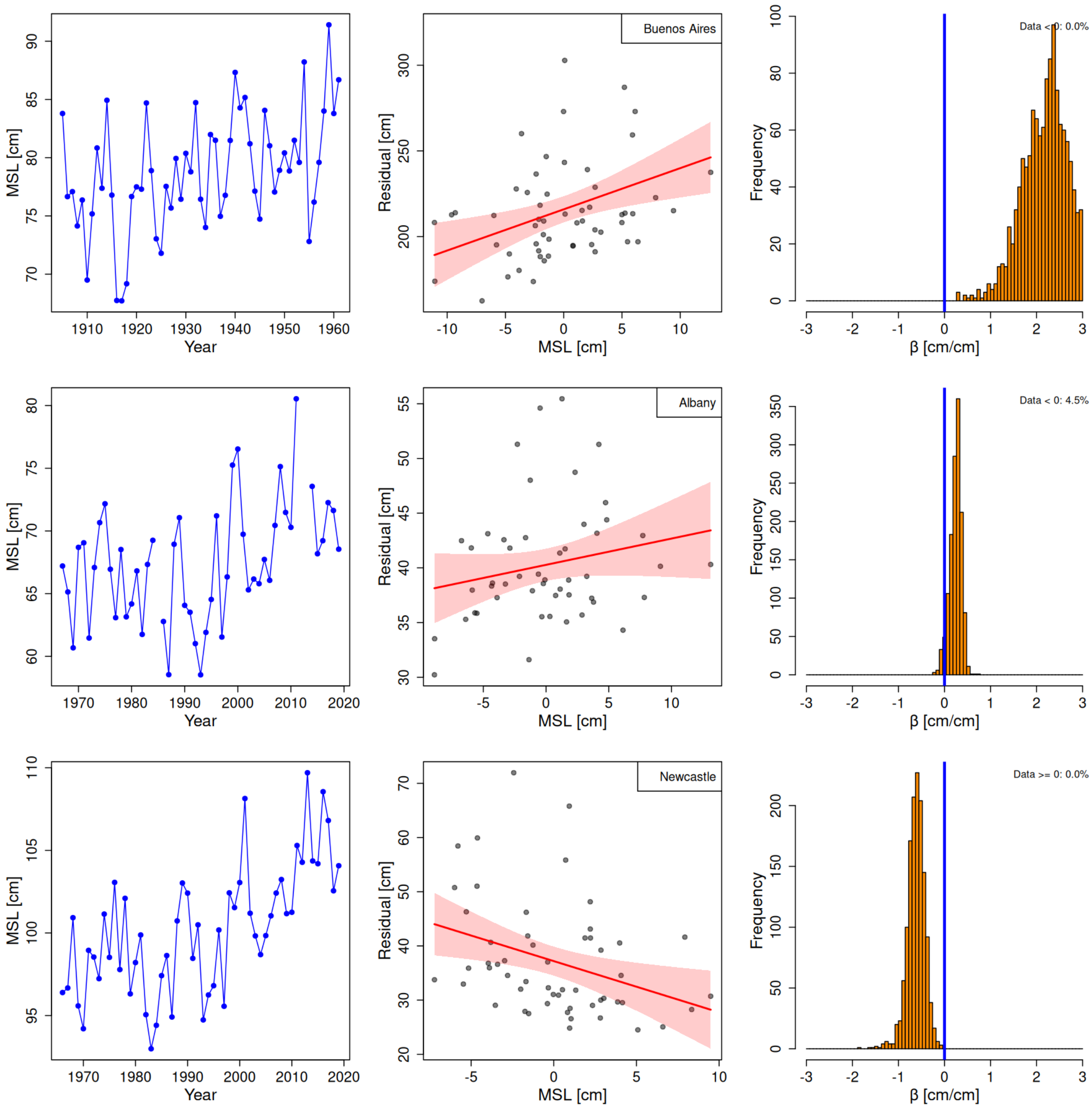

Figure 1: 3 of the statistically significant nonstationary series.

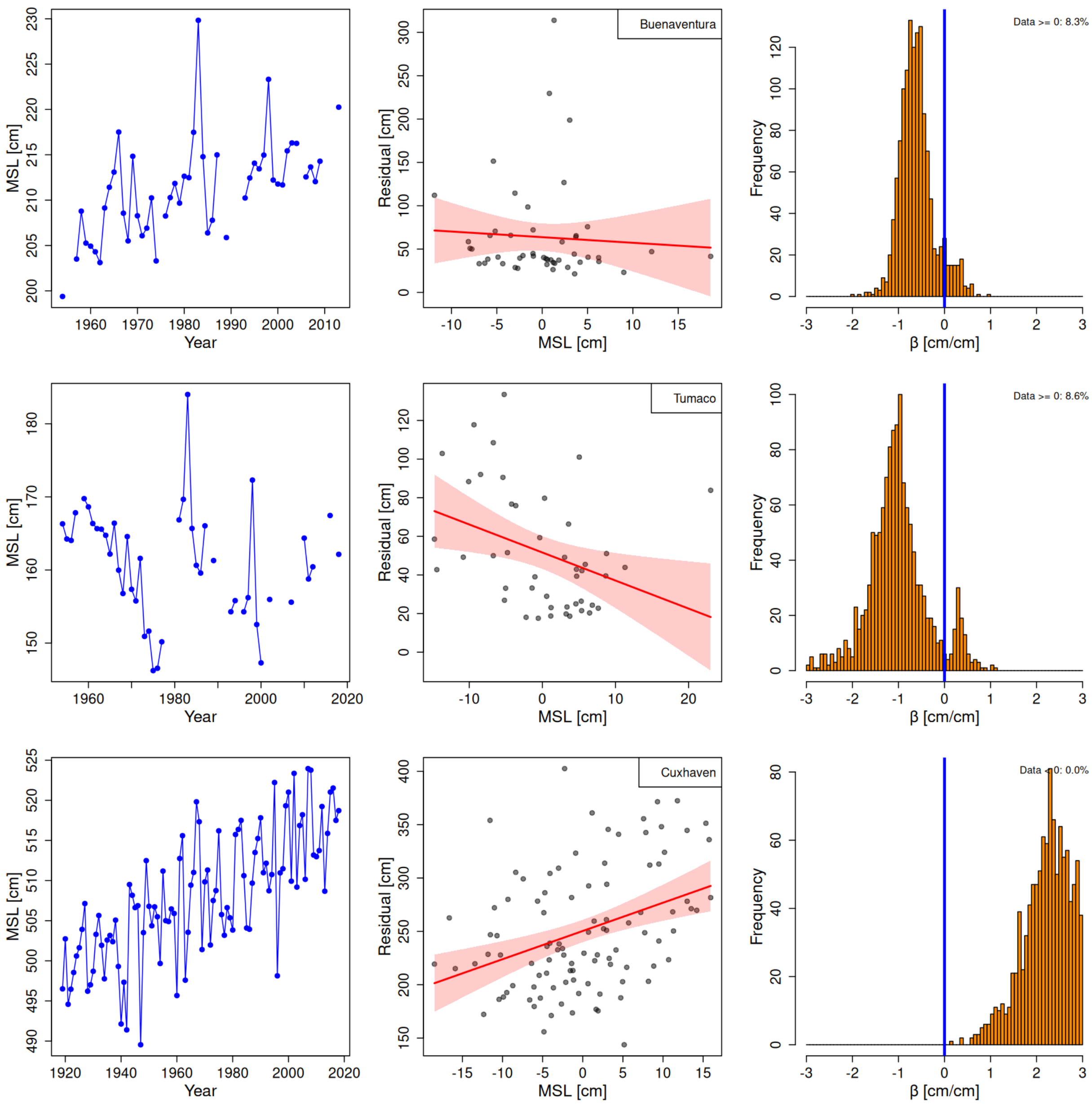

Figure 2: 3 of the statistically significant nonstationary series.

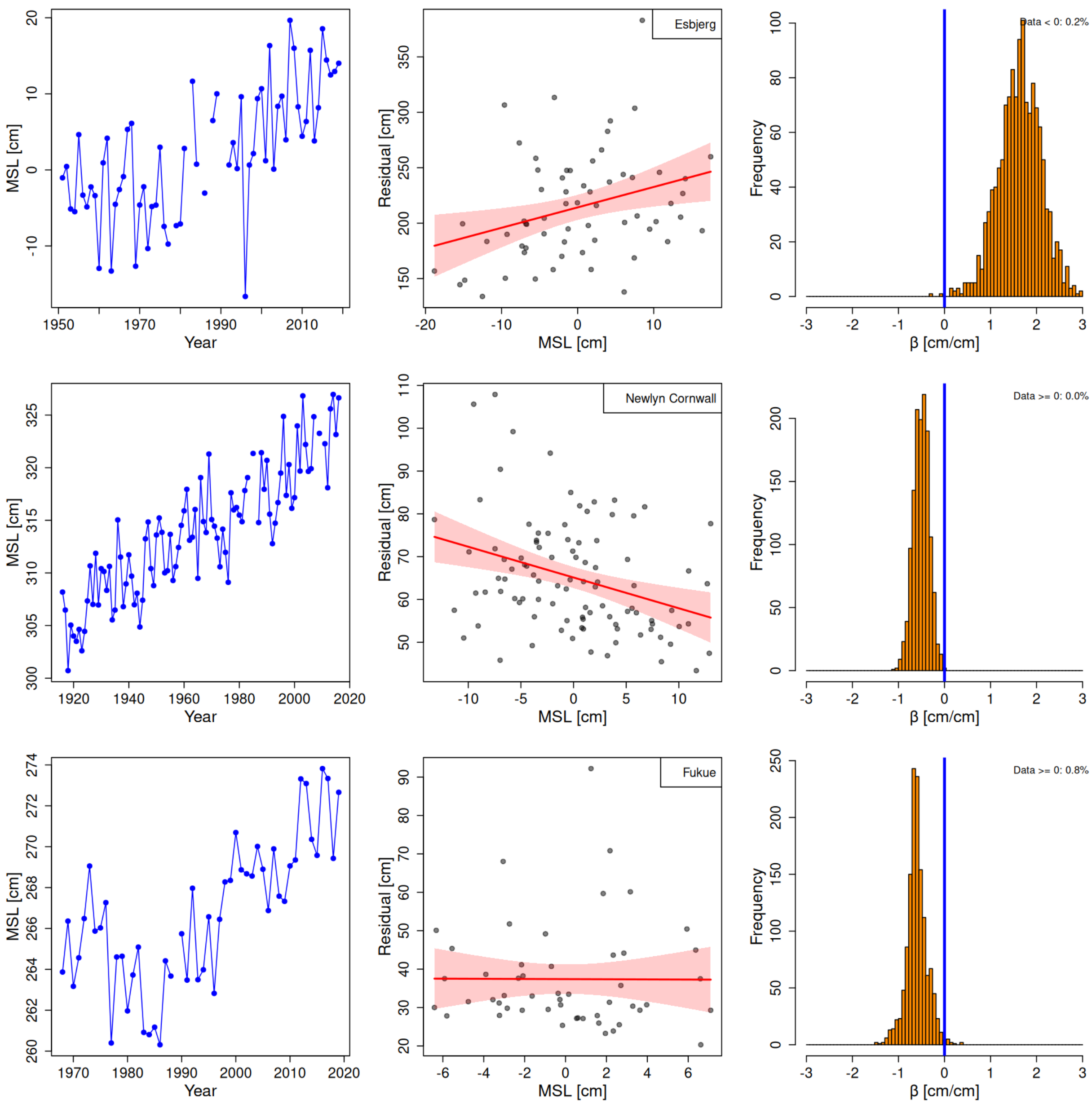

Figure 3: 3 of the statistically significant nonstationary series.

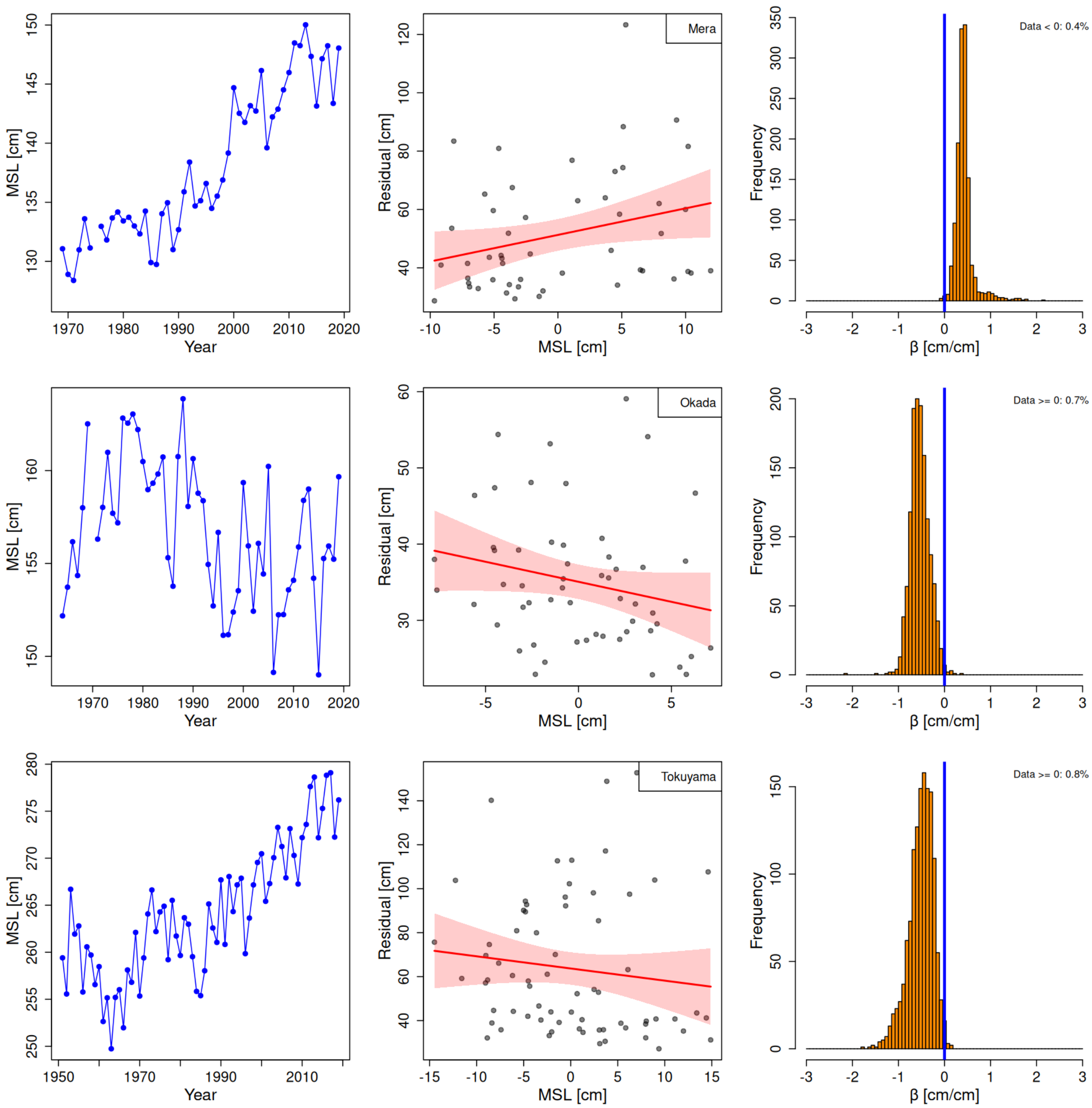

Figure 4: 3 of the statistically significant nonstationary series.

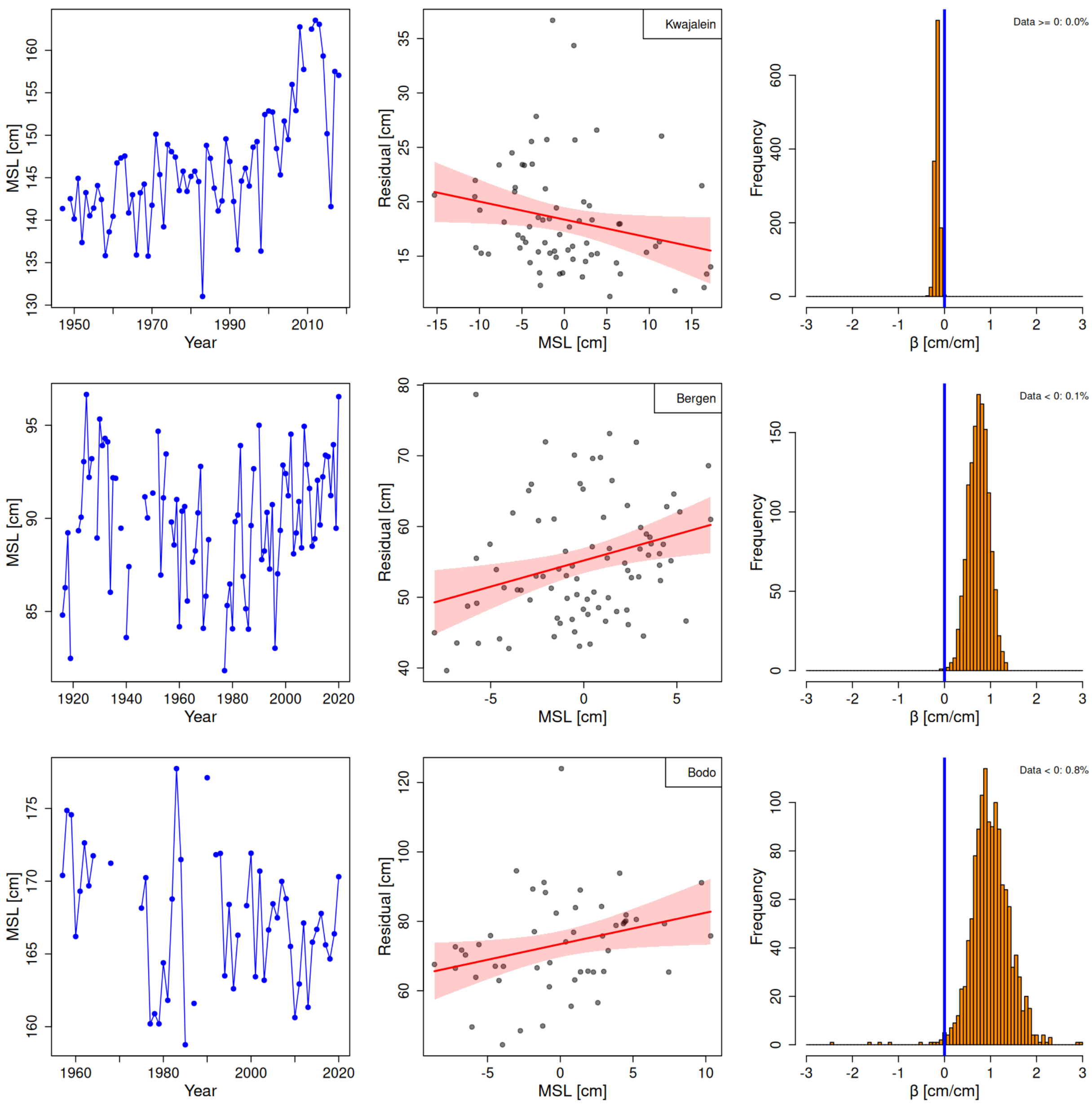

Figure 5: 3 of the statistically significant nonstationary series.

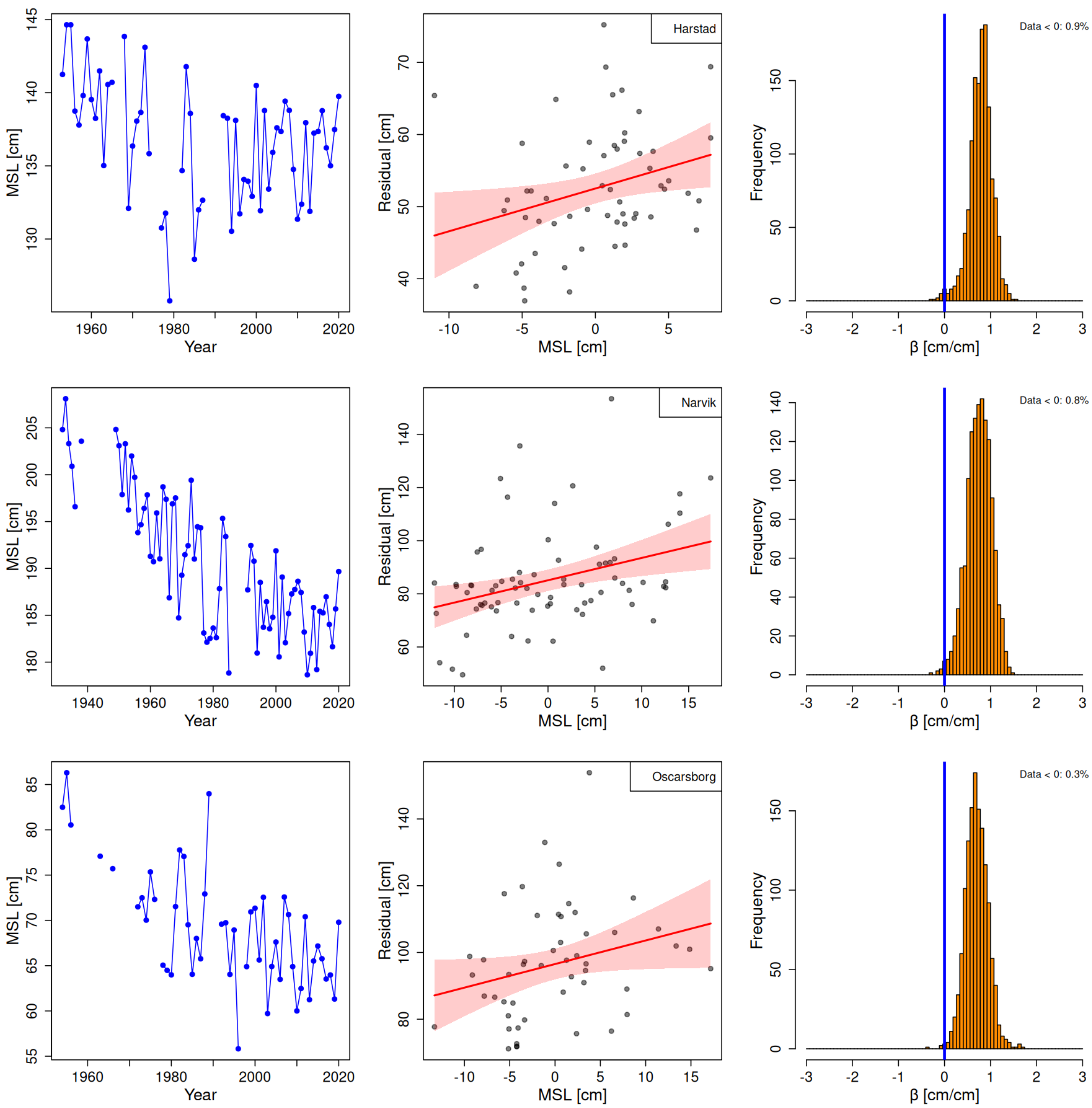

Figure 6: 3 of the statistically significant nonstationary series.

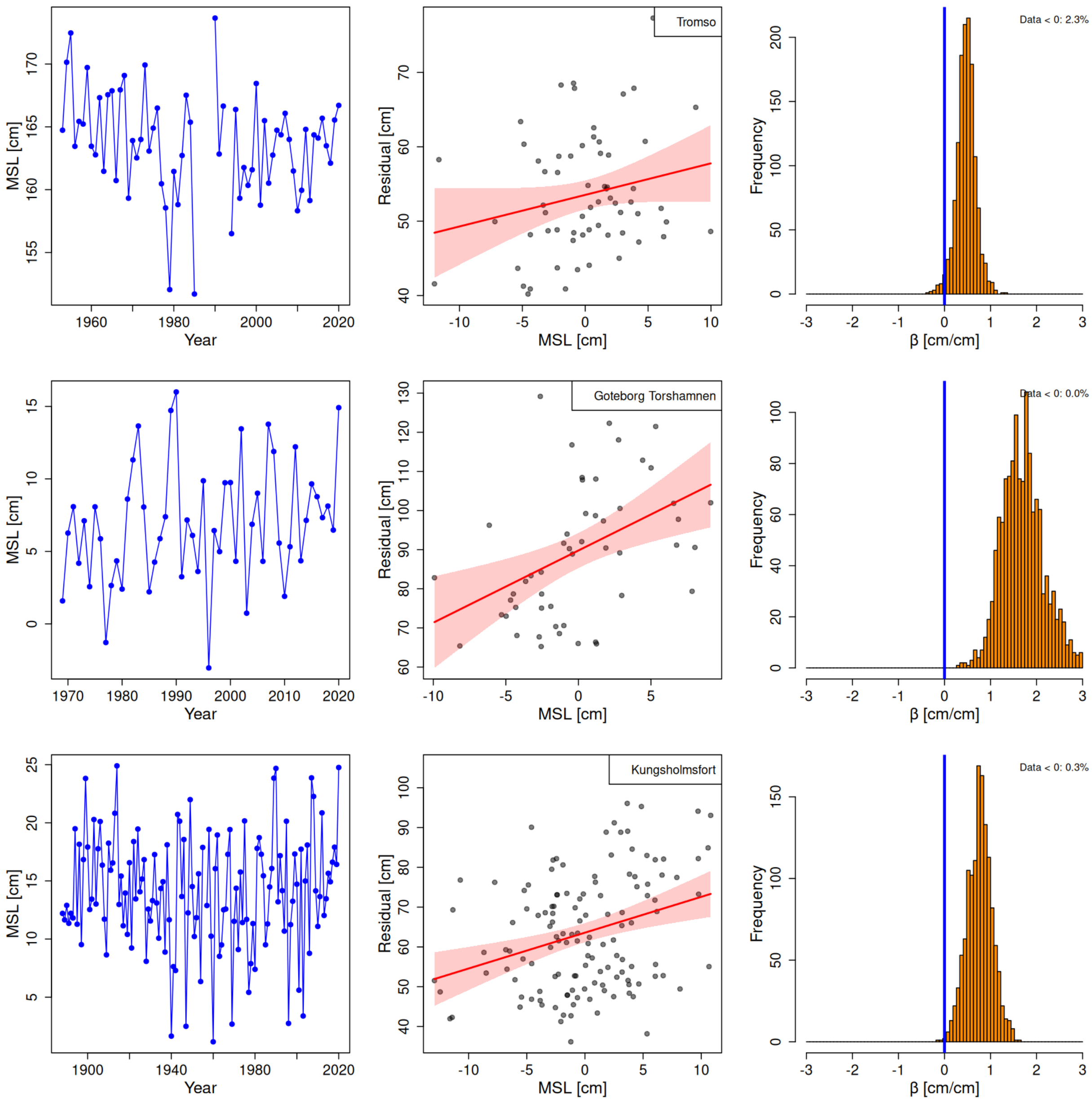

Figure 7: 3 of the statistically significant nonstationary series.

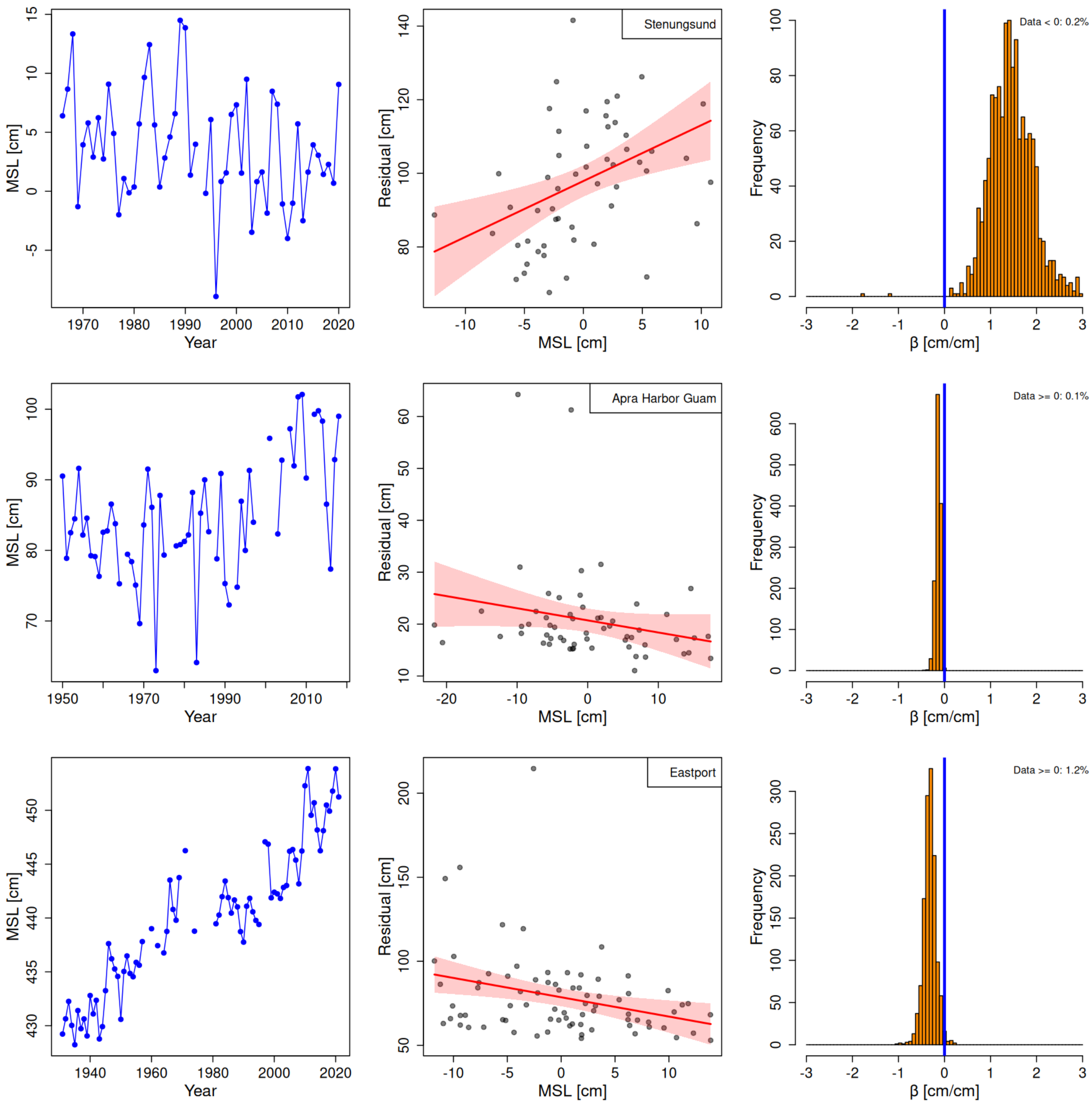

Figure 8: 3 of the statistically significant nonstationary series.

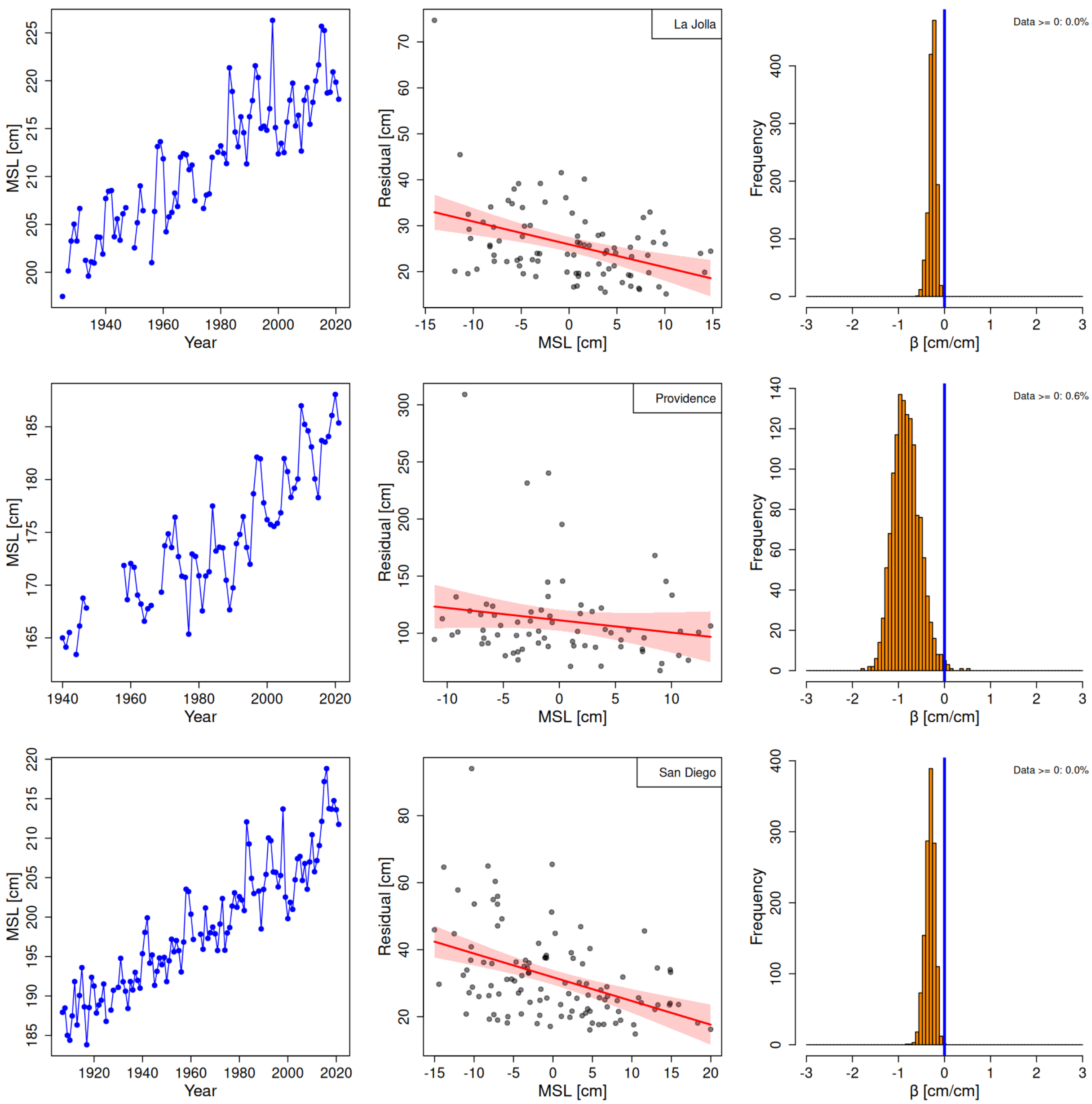

Figure 9: 3 of the statistically significant nonstationary series.

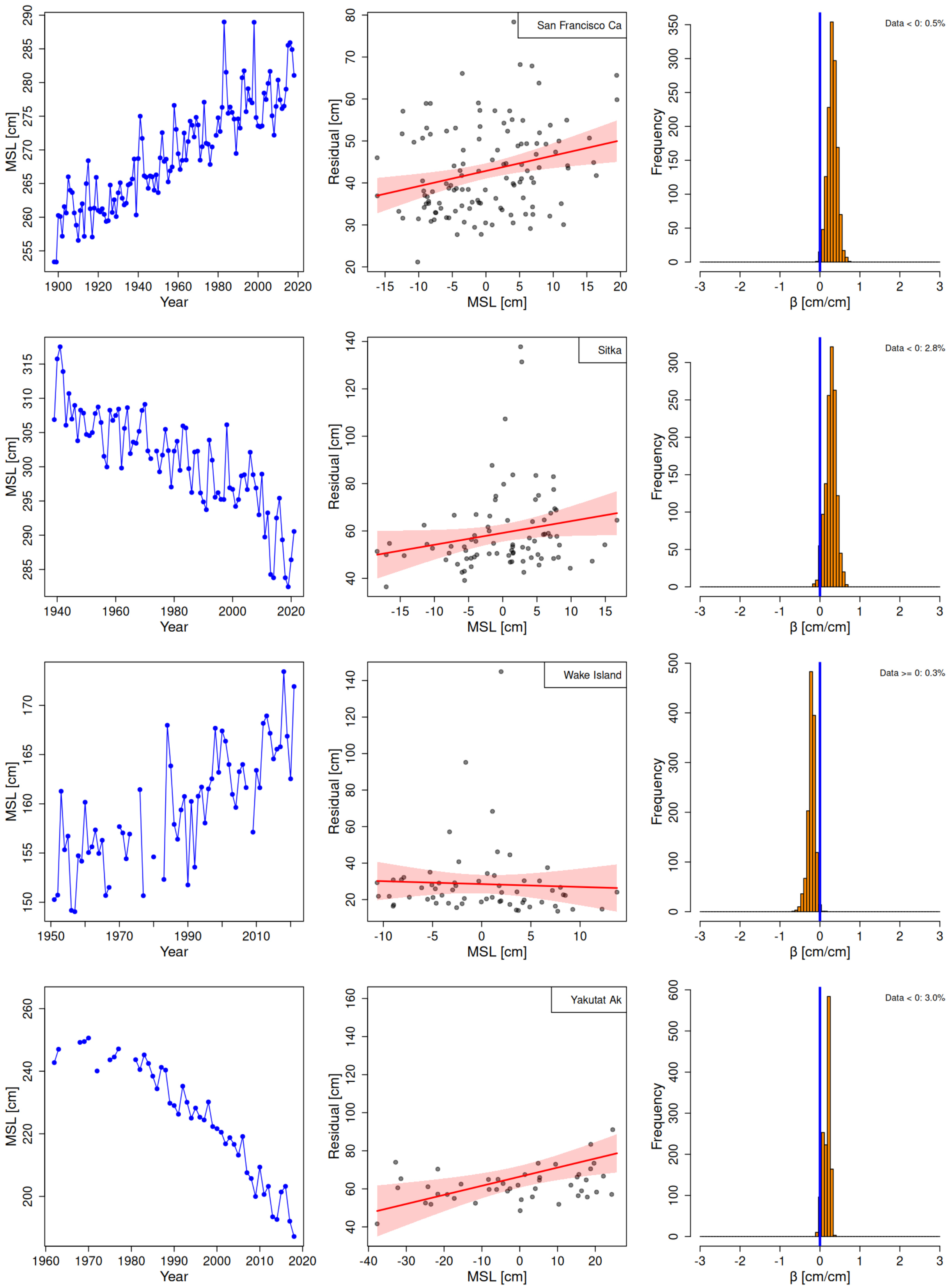

Figure 10: 3 of the statistically significant nonstationary series.

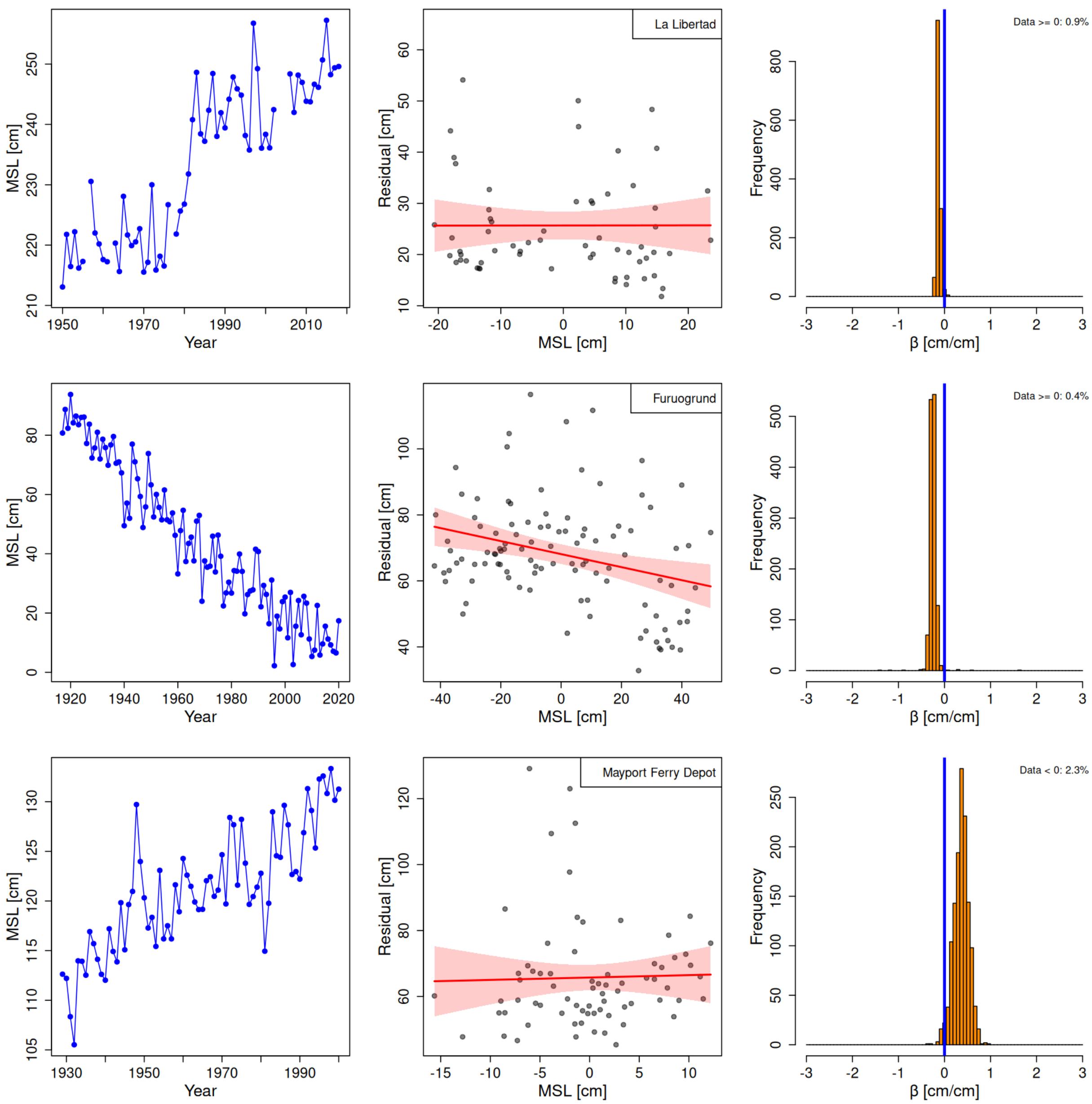

Figure 11: 4 of the statistically significant nonstationary series.

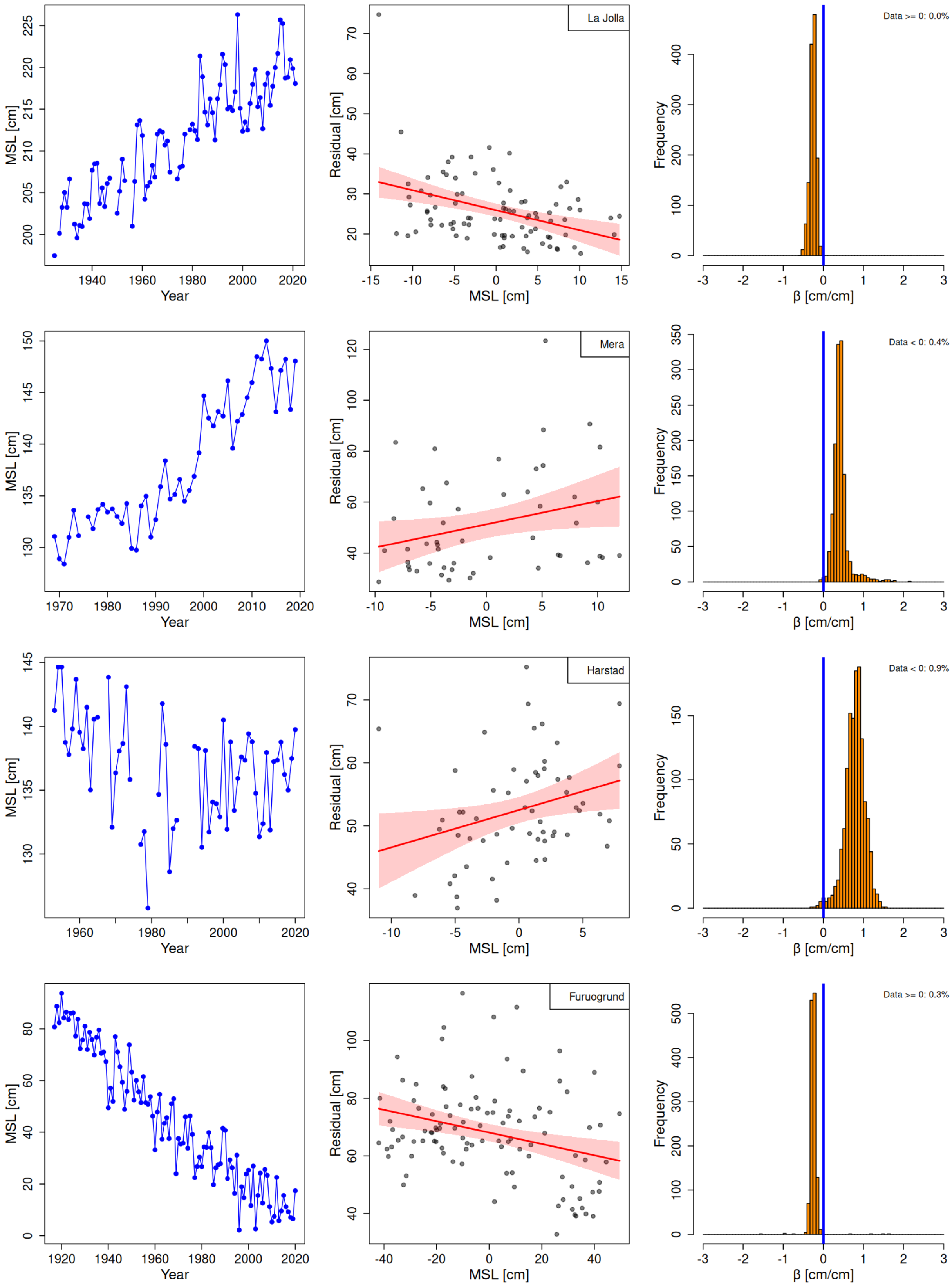

Figure 12: 4 illustrations of how oppositely MSL and extremes can co-evolve.

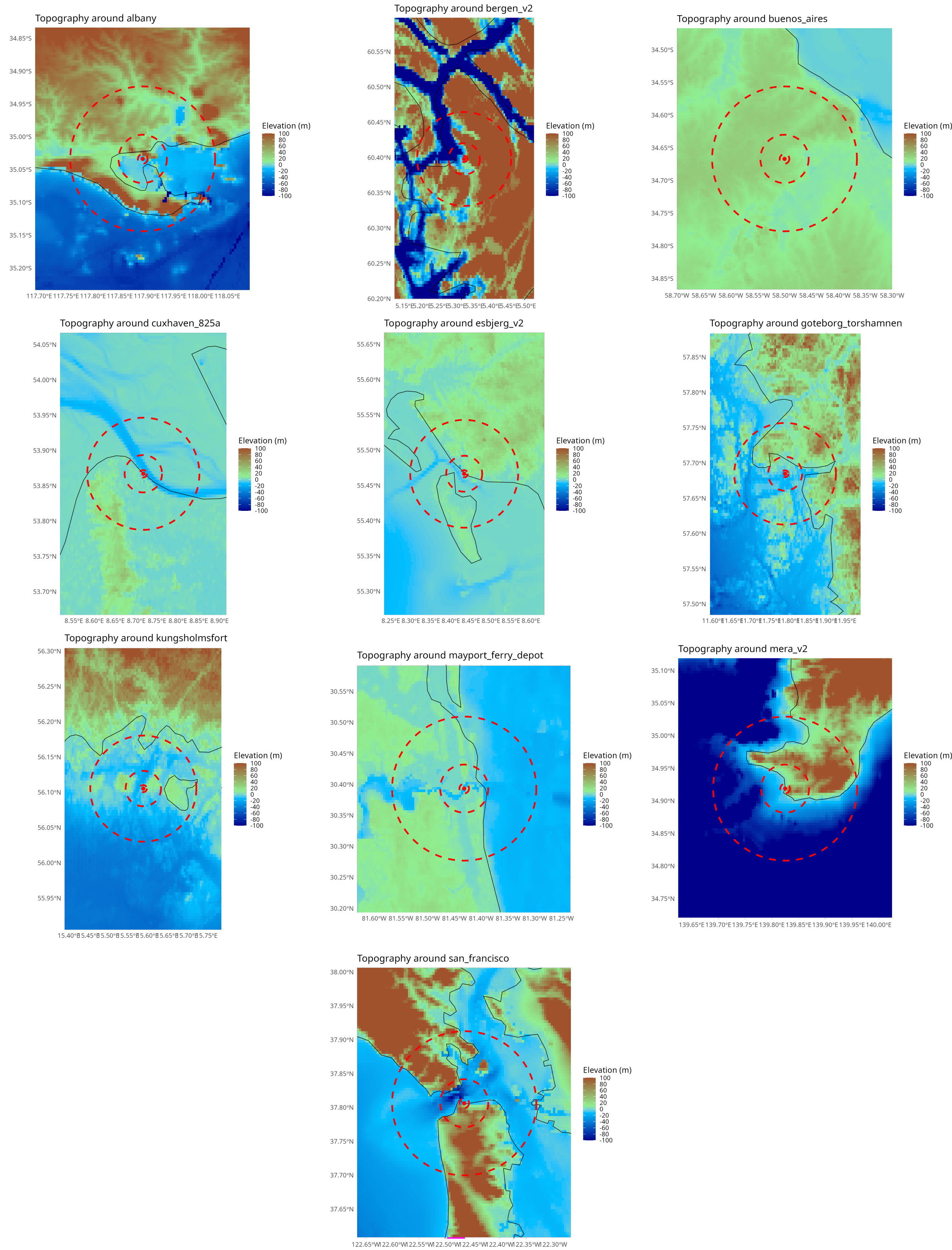

Figure 13: Station maps for the non-stationary stations with positive MSL trend and positive β.

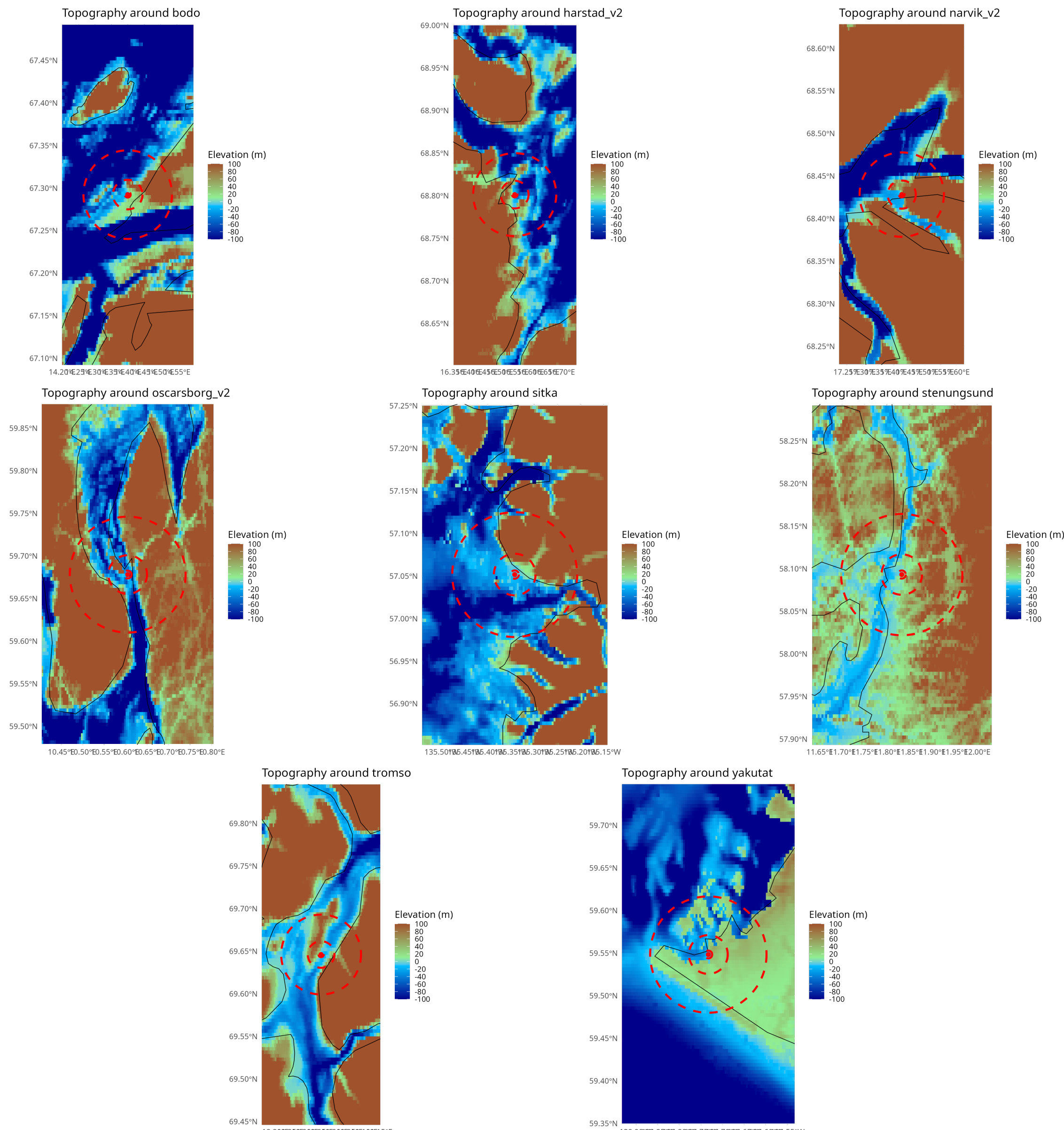

Figure 14: Station maps for the non-stationary stations with negative MSL trend and positive β.

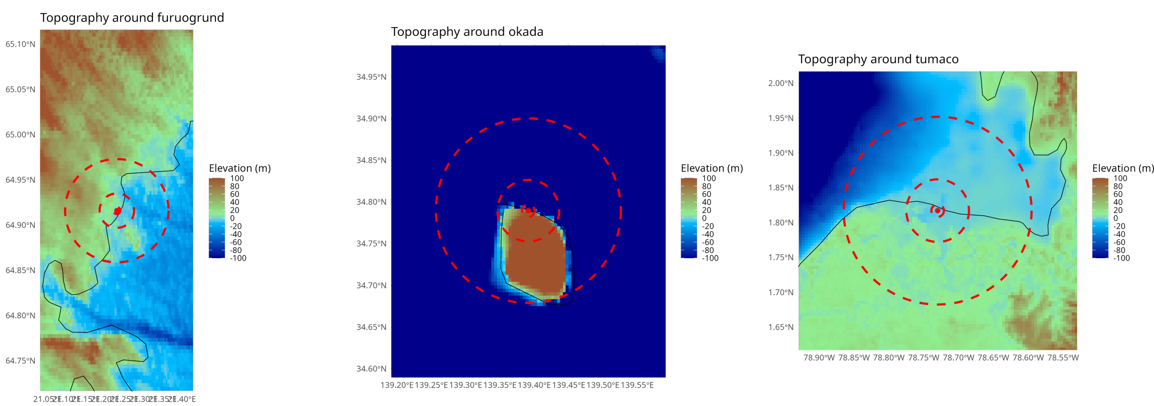

Figure 15: Station maps for the non-stationary stations with negative MSL trend and negative β.

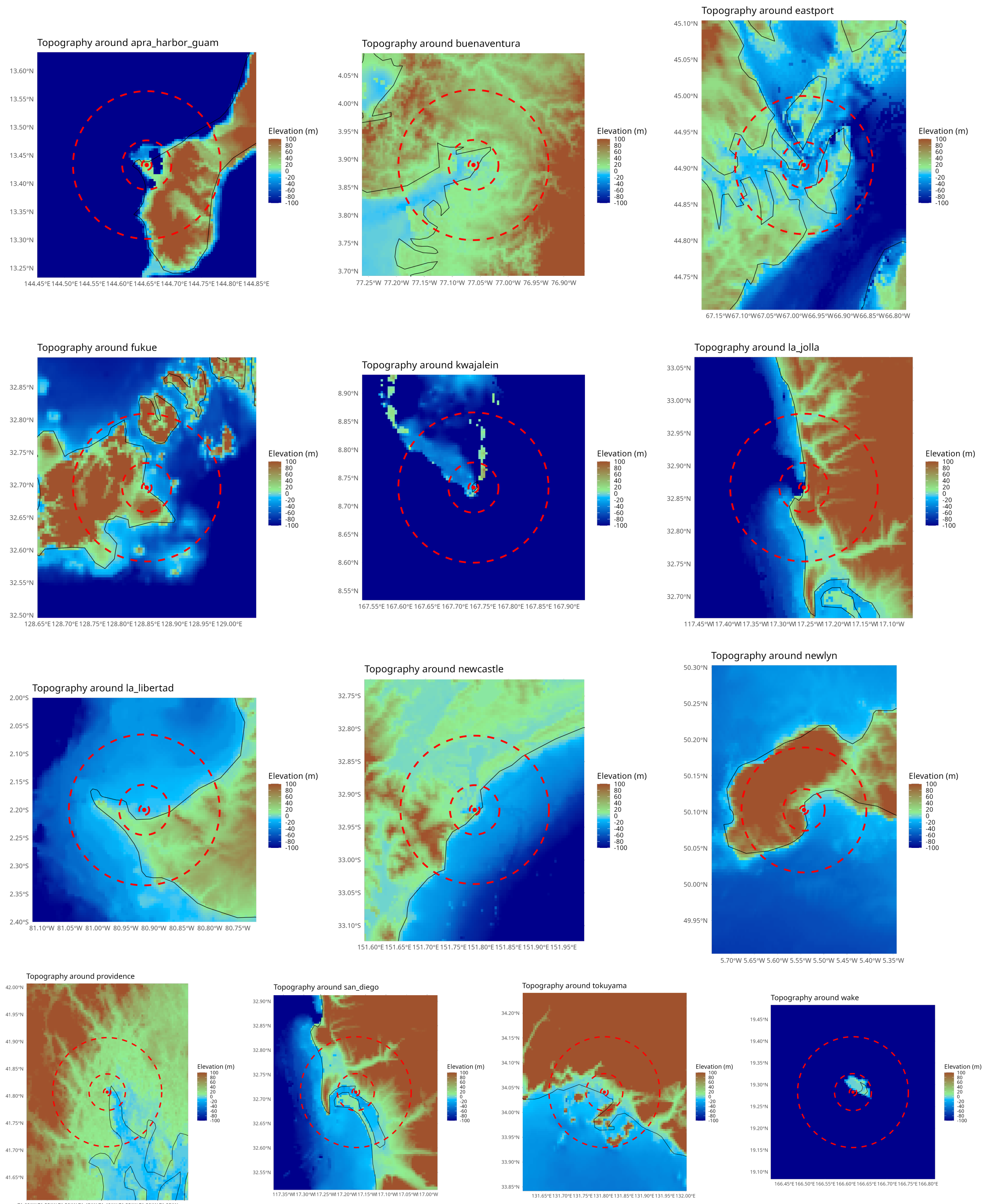

Figure 16: Station maps for the non-stationary stations with positive MSL trend and negative β.

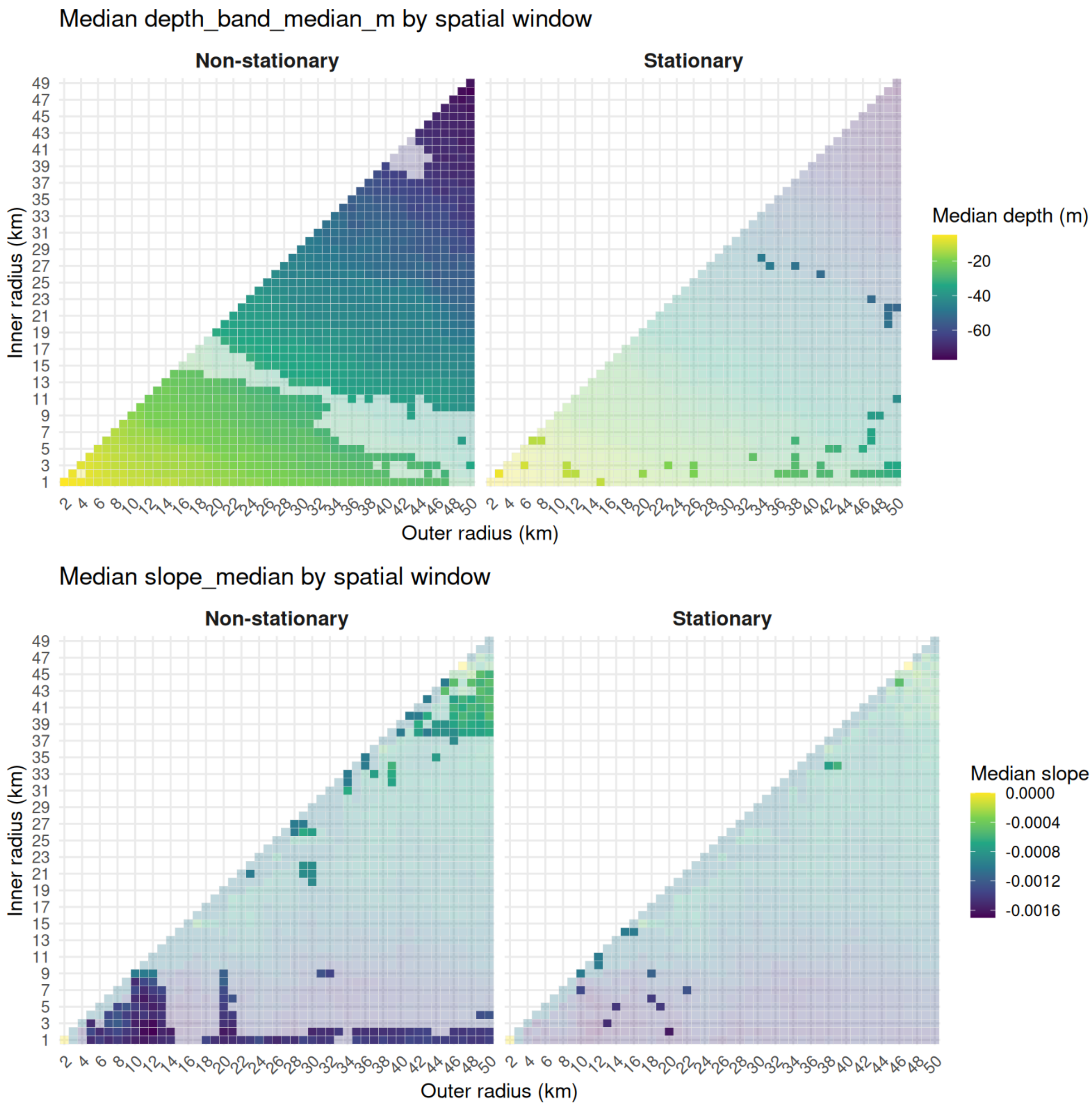

Figure 17: Median values of seabed depths and slopes at various annuli choices.

4. Distribution of MSL Slopes and β Coefficients

Supplementary Table 2:

MSL trend > 0, $\beta > 0$	**MSL trend > 0,** $\beta < 0$
Albany AUS	Apra Harbor Guam USA
Bergen NO	Buenaventura COL
Buenos Aires ARG	Eastport USA
Cuxhaven DE	Fukue JPN
Esbjerg DK	Kwajalein MHL
Goteborg Torshamnen SE	La Jolla USA
Kungsholmsfort SE	La Libertad ECU
Mayport Ferry Depot USA	Newcastle AUS
Mera JPN	Newlyn Cornwall UK
San Francisco USA	Providence USA
	San Diego USA
	Tokuyama JPN
	Wake Island USA
MSL trend < 0, $\beta > 0$	**MSL trend < 0,** $\beta < 0$
Bodo NOR	Furuogrund SE
Harstad NOR	Okada JPN
Narvik NO	Tumaco COL
Oscarsborg NO	
Sitka USA	
Stenungsund SE	
Tromso NO	
Yakutat USA	

Table 2: Joint distribution of signs of mean sea level (MSL) trends and covariate coefficients β for selected tide-gauge stations.